Journal of Organometallic Chemistry 630 (2001) 139–148

Journal of Organometallic Chemistry

www.elsevier.com/locate/jorganchem

Group 14 chalcogenides featuring a bicyclo[3.3.0]octane skeleton

U. Herzog [a,*], U. Böhme [a], E. Brendler [b], G. Rheinwald [c]

[a] *Institut für Anorganische Chemie der TU Bergakademie Freiberg, Leipziger Str. 29, D-09596 Freiberg, Germany*

[b] *Institut für Analytische Chemie der TU Bergakademie Freiberg, Leipziger Str. 29, D-09596 Freiberg, Germany*

[c] *Institut für Chemie, Lehrstuhl Anorganische Chemie, TU Chemnitz, Straße der Nationen 62, D-09111 Chemnitz, Germany*

Received 8 November 2000; accepted 21 May 2001

Abstract

Reactions of mixtures of $Cl_2MeSiSiMeCl_2$ (**1**) and Me_2MCl_2 (M = Si, Ge, Sn) with either H_2S/NEt_3 or Li_2E (E = Se, Te) yielded the bicyclo[3.3.0]octanes $Me_2M(E)_2Si_2Me_2(E)_2MMe_2$. A carbon containing analog, $(CH_2)_5C(S)_2Si_2Me_2(S)_2C(CH_2)_5$, was prepared from **1** and $(CH_2)_5C(SH)_2$. Crystal structures of three of these compounds were determined and the observed conformations of the bicyclo[3.3.0]octane skeletons compared with results of density functional theory calculations. Another class of silchalcogenides featuring a bicyclo[3.3.0]octane skeleton, $E(Me_2Si)_2Si_2Me_2(SiMe_2)_2E$, was formed from the doubly branched hexasilane $(ClMe_2Si)_2Si_2Me_2(SiMe_2Cl)_2$ and H_2S/NEt_3 or Li_2E. All products were characterized by multinuclear NMR (^1H, ^{13}C, ^{29}Si, ^{77}Se, ^{119}Sn, and ^{125}Te). © 2001 Elsevier Science B.V. All rights reserved.

Keywords: Group 14 chalcogenides; bicyclo[3.3.0]octane skeleton; density functional theory calculations

1. Introduction

The reaction of organochlorosilanes with either H_2E (E = S, Se) in the presence of a Lewis base or Li_2E (E = S, Se, Te) yields silicon chalcogenides which usually form four- or six-membered heterocycles or polycycles with adamantane [1] or double-decker [2,3] structures depending on the functionality of the starting chlorosilane and the steric demand of the organic substituents.

In our previous report on cyclic and polycyclic silthianes containing Si–Si bonds [4] we have shown that in this class of compounds five-membered heterocycles consisting of three silicon and two sulfur atoms are most stable. The reaction of Me_2SiCl_2 with H_2S/NEt_3 yields the six-membered ring compound $(Me_2SiS)_3$ and the analogous reaction of the disilane $ClMe_2Si–SiMe_2Cl$ results in the formation of the six-membered heterocycle $S(SiMe_2SiMe_2)_2S$ without any acyclic by-products. If, however the reaction with H_2S/NEt_3 is carried out with a mixture of the two chlorosilanes, a five-membered heterocyclic compound is formed preferably:

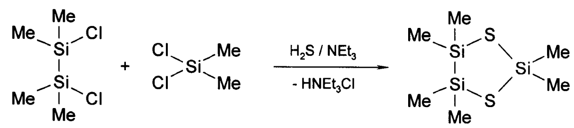

Density functional theory (DFT) calculations on the conversion reaction:

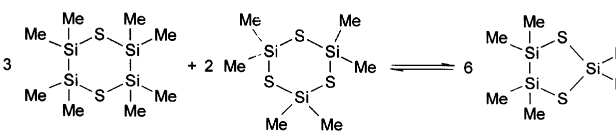

have indeed shown that the five-membered cyclic compound is 36 kJ mol^{-1} more stable than the corresponding mixture of the two six-membered heterocycles. This tendency also applies to systems with heavier Group 14 elements like germanium and tin and the heavier chalcogens selenium and tellurium. For instance the reaction of equimolar mixtures of Me_2MCl_2 (M = Ge, Sn) and $ClMe_2Si–SiMe_2Cl$ with Li_2Se or Li_2Te resulted in a selective formation of the five-membered heterocycles $Me_2M(E)_2Si_2Me_4$ [5]:

* Corresponding author. Tel.: + 49-3731-394-343; fax: + 49-3731-394-058.

E-mail address: herzog@merkur.brz.tu-freiberg.de (U. Herzog).

PII: S0022-328X(01)01010-5

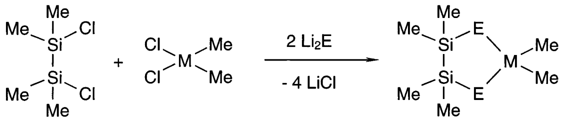

In continuation of these studies a mixture of the tetrafunctional disilane $Cl_2MeSi{-}SiMeCl_2$ (**1**) and Me_2SiCl_2 in a molar ratio of 1:2 is now shown to react with H_2S/NEt_2 yielding selectively 1,3,3,5,7,7-hexamethyl-2,4,6,8-tetrathiatetrasila-bicyclo[3.3.0]octane (**2a**):

The molecular structure of **2a** as determined by X-ray analysis revealed two fused five-membered rings adopting envelope conformations with one $SiMe_2$ unit in an *exo* and one in an *endo* position [4], see Fig. 1.

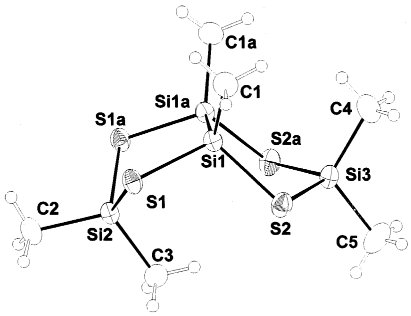

Fig. 1. ORTEP plot of the molecular structure of **2a** [4].

Table 1
NMR data (chemical shifts in ppm, coupling constants in Hz) of the bicyclo[3.3.0]octanes $R_2M(S)_2Si_2Me_2(S)_2MR_2$ (**2a**–**e**) ($MR_2 = SiMe_2$, $GeMe_2$, $SnMe_2$, $SnPh_2$, $C(CH_2)_5$)

compound	group	δ_M	δ_C	$^1J_{MC}$	δ_H
2a 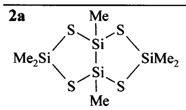	SiMe	29.85	5.2	52.2	0.91
	$SiMe_2$	35.3	7.5 / 8.2	58.7	0.66 / 0.73
2b 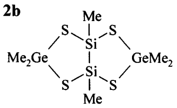	SiMe	33.2	5.6	51.5	0.87
	$GeMe_2$	-	10.4 / 10.5	-	0.95 / 1.03
2c 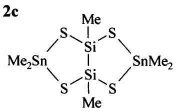	SiMe	29.8	6.4		0.94
	$SnMe_2$	181 $^2J_{SiSn}$ 10.2	3.5 / 4.8		0.79 / 0.87
2d 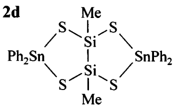	SiMe	31.4	6.2 $^3J_{SnC}$: 16.8	49.8	0.83
	$SnPh_2$	56 $^2J_{SiSn}$ 8.8	a)		7.35 (8 H), 7.58 (12 H)
2e 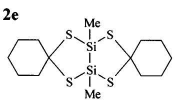	SiMe	33.1	1.15		0.92
	$\underline{C}(CH_2)_5$	74.4	b)		b)

a) Ph ^{13}C: i 139.2 ($^1J_{SnC}$: 644.8) / 139.5 ($^1J_{SnC}$: 612.0), o 135.15 ($^2J_{SnC}$ 51.9) / 135.5 ($^2J_{SnC}$ 55.9), m 128.6 ($^3J_{SnC}$ 71.9) / 128.9 ($^3J_{SnC}$ 67.1), p 130.0 ($^4J_{SnC}$ 15.2) / 130.2 ($^4J_{SnC}$ 14.3),
b) Cyclohexane rings ^{13}C: o 44.2 / 47.7, m 23.9 / 24.1, p 24.9; ^{1}H: o 2.03 / 2.26, m 1.65 / 1.70, p 1.42

The aim of this work is to extend these investigations to bicyclo[3.3.0]octanes also containing other Group 14 elements (C, Ge, Sn) and/or heavier chalcogens (Se, Te).

2. Results and discussion

2.1. Formation of 2,4,6,8-tetrachalcogena-bicyclo[3.3.0]octanes

Reacting 1:2 mixtures of **1** and the dichloro compounds Me_2MCl_2 (M = Ge, Sn) or Ph_2SnCl_2 with H_2S/NEt_3 the corresponding bicyclo[3.3.0]octanes **2b**–**d** are formed in high yields:

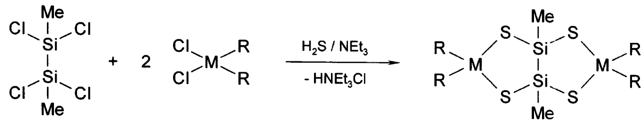

2b : $MR_2 = GeMe_2$
2c : $MR_2 = SnMe_2$
2d : $MR_2 = SnPh_2$

The carbon containing derivative **2e** could be prepared by treatment of **1** with two equivalents of cyclohexane-1,1-dithiol which had been prepared from cyclohexanone and H_2S according to Ref. [6]:

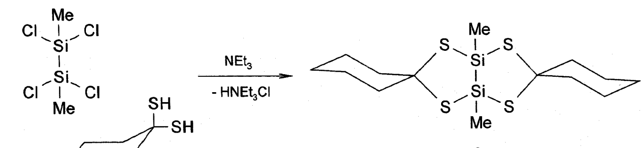

2e

Analogous selenium and tellurium containing bicyclo[3.3.0]octanes (**3a**–**c**, **4a**–**c**) have been synthesized by analogous reactions of mixtures of **1** and Me_2MCl_2 (M = Si, Ge, Sn) with either Li_2Se or Li_2Te in THF solution:

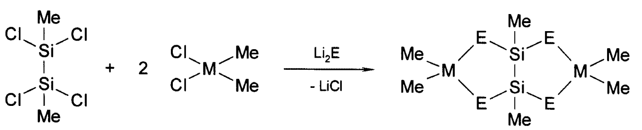

3a : E = Se, M = Si; **4a** : E = Te, M = Si
3b : E = Se, M = Ge; **4b** : E = Te, M = Ge
3c : E = Se, M = Sn; **4c** : E = Te, M = Sn

All newly prepared 2,4,6,8-tetrachalcogena-bicyclo[3.3.0]octanes are colorless solids. Their stability towards moisture and air decreases dramatically from the sulfur via the selenium to the tellurium heterocycles. Nevertheless all compounds could be characterized by multinuclear NMR spectroscopy, see Tables 1 and 2, and in some cases by GC–MS.

Table 2
NMR data (chemical shifts in ppm, coupling constants in Hz) of the bicyclo[3.3.0]octanes $Me_2M(E)_2Si_2Me_2(E)_2MMe_2$ (**3a**–**4c**) (M = Si, Ge, Sn; E = Se, Te)

compound	δ_E	group	δ_M	$^1J_{ME}$	δ_C	$^1J_{MC}$	δ_H
3a 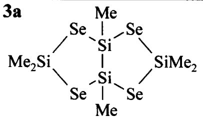	-208	SiMe	32.6	138.5	6.0		1.07
				$^2J_{SiSe}$ 10.2			
		$SiMe_2$	28.7	128.3	7.7 / 9.3	53.9	0.88 / 0.95
3b 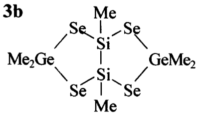	-217	SiMe	35.8	144.3	5.9		1.02
				$^2J_{SiSe}$ 9.7			
		$GeMe_2$			11.53 / 11.58	-	1.15 / 1.21
3c 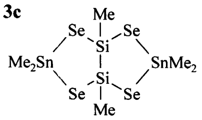	-378	SiMe	31.1	143.2	6.3		1.04
				$^2J_{SiSe}$ 10			
		$SnMe_2$	114.4	1149	3.6 /	336.4	0.94 /
				$^2J_{SiSn}$ 14.1	4.7	362.8	0.96
4a 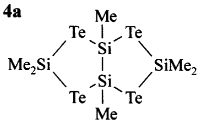	-650	SiMe	11.9	369.8	5.1		1.30
				$^2J_{SiTe}$ 40.3			
		$SiMe_2$	-23.7	345.0	9.5 / 10.8		1.22
4b 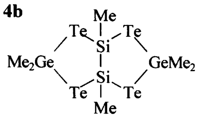	-645	SiMe	14.9	380.5	5.0		1.22
				$^2J_{SiTe}$ 40.8			
		$GeMe_2$			11.5 / 12.5	-	1.47 / 1.50
4c 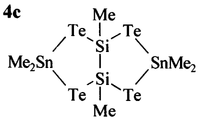	-913	SiMe	7.8	372.7			1.23
				$^2J_{SiTe}$ 43.2			
		$SnMe_2$	-72	2927			1.19
				$^2J_{SiSn}$ 8.7			

While the chemical shifts of M (C, Si, Sn) in the MR_2 units of **2a**–**4c** are similar to those of the corresponding five-membered monocyclic compounds $Me_4Si_2(E)_2MR_2$ [5] (in most cases slightly shifted to lower field), the selenium and tellurium resonances are observed by 60–105 ppm further downfield. Due to the bicyclic systems in **2a**–**4c** the two organic substituents at M are diastereotopic giving rise to two different ^1H- and ^{13}C-NMR signals.

2.2. Molecular structures of 2,4,6,8-tetrachalcogena-bicyclo[3.3.0]octanes

X-ray structure analyses have been carried out for **2b**, **2e** and **3c** while the molecular structure of **2a** has been reported previously [4]. Figs. 2–4 show the molecular structures. Compounds **2a** and **2b** crystallize in the same space group with almost identical unit cell parameters (Tables 3–5).

While the bicyclo[3.3.0]octane skeletons of **2a**, **2b** and **2e** adopt a bis-envelope conformation, it is obvious that a rather twisted conformation of both five-membered rings is observed for **3c**. The reasons for this different conformation could be the larger bond lengths of Sn–Se as well as Se–Si whereas the central Si–Si bond remains the same.

Comparing the geometries of **2e**, **2a** and **2b** it can be seen that in this series of compounds with the ring atoms M (C, Si, Ge) the Si–Si bond length increases from 2.328(1) (**2e**) via 2.360(1) (**2a**) to 2.367(1) (**2b**). Consistently the average bond angles Si–S–M (101.99 ° in **2e**, 99.12 ° in **2a**, 98.72 ° in **2b**) and S–M–S (112.31 ° in **2e**, 107.91 ° in **2a**, 105.28 ° in **2b**)

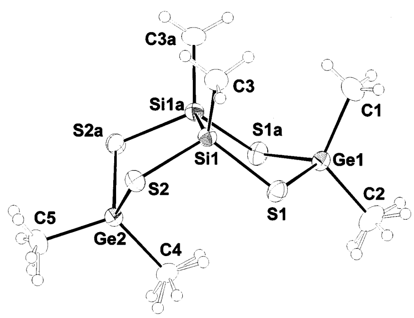

Fig. 2. Molecular structure of **2b**.

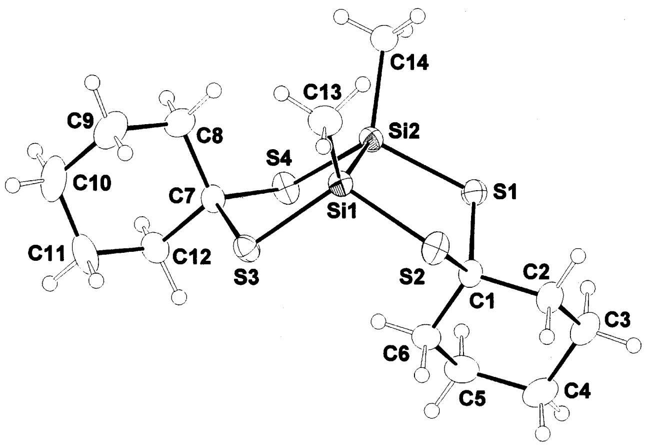

Fig. 3. Molecular structure of **2e**.

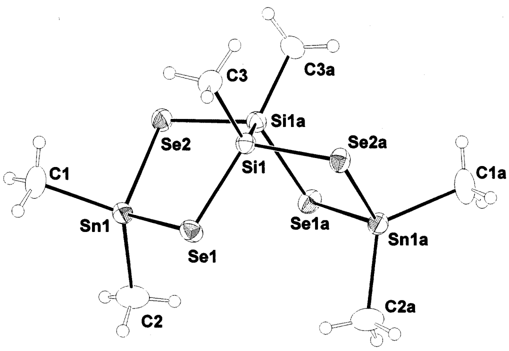

Fig. 4. Molecular structure of **3c**.

Table 3
Selected bond distances and angles of **2b**

Atoms	Distances (Å)	Atoms	Angles (°)
Si(1)–Si(1a)	2.3672(9)	S(1)–Si(1)–S(2)	109.80(2)
S(1)–Si(1)	2.1422(6)	S(1)–Si(1)–Si(1a)	106.58(2)
S(2)–Si(1)	2.1317(6)	S(2)–Si(1)–Si(1a)	105.89(2)
S(1)–Ge(1)	2.2360(5)	Si(1)–S(1)–Ge(1)	98.87(2)
S(2)–Ge(2)	2.2457(4)	Si(1)–S(2)–Ge(2)	98.58(2)
Si(1)–C(3)	1.859(2)	S(1)–Ge(1)–S(1a)	106.77(2)
Ge(1)–C(1)	1.928(3)	S(2)–Ge(2)–S(2a)	103.79(2)
Ge(1)–C(2)	1.931(3)	C(1)–Ge(1)–C(2)	115.91(14)
Ge(2)–C(4)	1.933(2)	C(4)–Ge(2)–C(5)	115.31(11)
Ge(2)–C(5)	1.929(2)		

decrease while the average angles Si–Si–S increase from 100.33 (**2e**) via 105.16 ° (**2a**) to 106.24 ° (**2b**). This is attributed to an increase in the bond lengths S–C, S–Si, S–Ge. The angles between the planes Si_2S_2 and S_2M which characterize the envelope conformation of the related heterocycles vary only slightly between 49 and 50 °.

In order to get a better understanding of these differences we have performed DFT calculations on the bicyclo[3.3.0]octanes $Me_2C(S)_2Si_2Me_2(S)_2CMe_2$ (**2f**) as a model for **2e**, **2a**, **2b**, **2c** and **3c**. For **2f**, **2a** and **2b** two conformations were found as minima, one with the experimentally observed bis-envelope conformation and one with a twisted conformation similar to that observed for **3c**. For the tin compounds (**2c** and **3c**) only one minimum corresponding to the twist conformation could be found. Whereas for **2f** the bis-envelope conformation is definitely more stable by 7.4 kJ mol^{-1} the differences for **2a** are very small (0.4 kJ mol^{-1}, see also Table 6 and Fig. 5) and for **2b** the twist conformation is 3.65 kJ mol^{-1} lower in energy.

These calculations suggest, that in solution both conformations of **2a** are present. Indeed, a ^{29}Si-CP-MAS-NMR spectrum of the crystalline compound **2a** shows significant differences of the chemical shift values (27.0 ppm for the central Si_2Me_2 unit and 36.4/31.7 ppm for the two $SiMe_2$ units) from those obtained from solution (Table 1), even if one compares the average value of the two crystallographic different $SiMe_2$ units, see Fig. 6.

On the other hand, a ^{29}Si-CP-MAS-NMR spectrum of $S(SiMe_2\text{-}SiMe_2)_2S$ revealed two signals at −4.83 and −4.56 ppm. This observation is in accordance with the crystal structure analysis [5] showing two crystallographically different silicon atoms while in solution a very similar ^{29}Si-NMR chemical shift of −4.76 ppm was observed [5]. Here, the six-membered heterocycle adopts a chair conformation in solution as well as in the solid state.

Table 4
Selected bond distances and angles of **2e**

Atoms	Distances (Å)	Atoms	Angles (°)
Si(1)–Si(2)	2.3275(7)	S(1)–Si(2)–S(4)	112.89(3)
S(1)–Si(2)	2.1330(7)	S(2)–Si(1)–S(3)	113.57(3)
S(2)–Si(1)	2.1378(7)	Si(1)–Si(2)–S(1)	100.58(3)
S(3)–Si(1)	2.1463(7)	Si(1)–Si(2)–S(4)	100.32(3)
S(4)–Si(2)	2.1486(7)	Si(2)–Si(1)–S(2)	100.17(3)
S(1)–C(1)	1.863(2)	Si(2)–Si(1)–S(3)	100.26(3)
S(2)–C(1)	1.865(2)	Si(1)–S(2)–C(1)	103.11(6)
S(3)–C(7)	1.864(2)	Si(2)–S(1)–C(1)	103.59(6)
S(4)–C(7)	1.864(2)	Si(1)–S(3)–C(7)	100.46(6)
Si(1)–C(13)	1.863(2)	Si(2)–S(4)–C(7)	100.79(6)
Si(2)–C(14)	1.863(2)	S(1)–C(1)–S(2)	112.37(10)
		S(3)–C(7)–S(4)	112.25(10)

Table 5
Selected bond distances and angles of **3c**

Atoms	Distances (Å)	Atoms	Angles (°)
Si(1)–Si(1a)	2.333(2)	Se(1)–Si(1)–Se(2a)	109.51(4)
Si(1)–Se(1)	2.2802(10)	Si(1a)–Si(1)–Se(1)	105.84(4)
Si(1)–Se(2a)	2.2751(10)	Si(1)–Si(1a)–Se(2)	106.88(6)
Sn(1)–Se(1)	2.5546(5)	Si(1)–Se(1)–Sn(1)	98.61(3)
Sn(1)–Se(2)	2.5566(4)	Si(1a)–Se(2)–Sn(1)	96.39(3)
Si(1)–C(3)	1.861(4)	Se(1)–Sn(1)–Se(2)	107.79(1)
Sn(1)–C(1)	2.119(4)	C(1)–Sn(1)–C(2)	120.3(2)
Sn(1)–C(2)	2.126(4)		

Table 6
Results of the DFT calculations on $Me_2M(S)_2Si_2Me_2(S)_2MMe_2$ (**2f**, **a**–**c**; M = C, Si, Ge, Sn) and $Me_2Sn(Se)_2Si_2Me_2(Se)_2SnMe_2$ (**3c**)

Compound	**2f**		**2a**		**2b**		**2c**	**3c**
M	C		Si		Ge		Sn	Sn
Conformation	Bis-envelope	Twist	Bis-envelope	Twist	Bis-envelope	Twist	Twist	Twist
Total energy (H)	−2487.59397	−2487.59096	−2990.56098	−2990.56125	−2419.04330	−2419.04480	−2418.25497	−862.39606
Total energy with zero point correction (H)	−2487.34091	−2487.33809	−2990.32305	−2990.32320	−2418.80780	−2418.80919	−2418.02269	−862.16696
Si–Si (Å)	2.352	2.326	2.381	2.353	2.393	2.360	2.365	2.371
Si–S (Å)	2.175, 2.158	2.160, 2.174	2.178, 2.165	2.180, 2.166	2.178, 2.163	2.180, 2.165	2.165, 2.185	2.333, 2.353
M–S (Å)	1.884, 1.884	1.875, 1.900	2.184, 2.178	2.189, 2.179	2.282, 2.289	2.297, 2.284	2.445, 2.455	2.631, 2.639
Si–S–M (°)	101.6, 102.8	107.1, 103.7	100.3, 101.0	105.0, 101.2	100.3, 101.8	104.4, 100.1	103.5, 99.1	100.8, 96.7

If both conformations of **2a** were present in solution, the NMR data of **2a** should be temperature dependent since lower temperature would favor the more stable conformation. Indeed, both the ^{29}Si- and the ^{1}H-NMR spectra show changes with temperature (Fig. 7a,b). Only one of the two $SiMe_2$ proton resonances (A) does not vary significantly with temperature, probably due to identical chemical shift values in both conformations.

For the germanium compound **2b** there is a contradiction between the results of the DFT calculation and the observed molecular structure. Here, crystal packing forces probably stabilize the bis-envelope conformation. On the other hand, the structure of the tin and selenium containing compound **3c** is again in accordance with the result of the calculations. However, it must be noted that there are additional but weak intermolecular contacts between selenium and tin atoms. The interatomic distances are, with values between 4.0 and 4.1 Å, slightly below the sum of the van-der-Waals radii of 4.2 Å, also see Fig. 8. These intermolecular contacts lead to the formation of wavy sheets of silicon, selenium and tin atoms perpendicular to the crystallographic *b*-axis.

Taking into account these intermolecular contacts the coordination number of selenium increases to three with a sum of the three bond angles of 322.6 ° at Se1 and 318.5 ° at Se2 and that of tin reaches six. The coordination sphere at tin can be regarded as a doubly capped tetrahedron characterized by Se1–Sn1–Se1b and Se2–Sn1–Se2b angles of 175.0 and 166.8 °, respectively. Such intramolecular contacts have already been reported for other tin selenium compounds, for example in $Me_2Sn(Se)_2Sn_2Me_4$, here the five-membered Sn_3Se_2 heterocycle adopts an envelope conformation and intermolecular Sn–Se contacts of 3.76–4.09 Å are

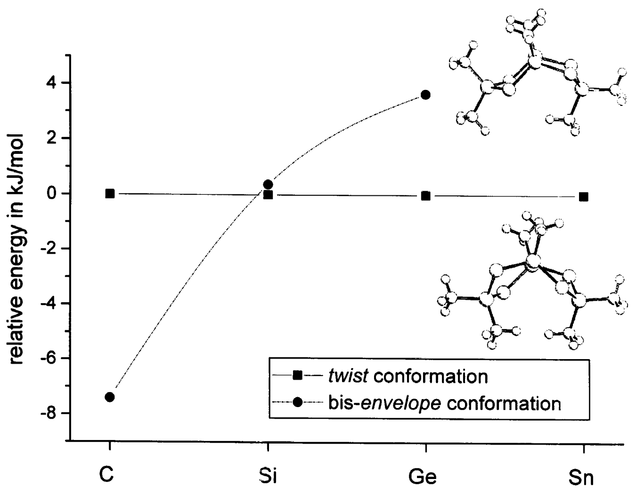

Fig. 5. Relative stabilities of the bis-envelope and twist conformations of $Me_2M(S)_2Si_2Me_2(S)_2MMe_2$, **2f**, **2a**–**c** (M = C, Si, Ge, Sn) as obtained from DFT calculations at the level B3LYP/6-31G*.

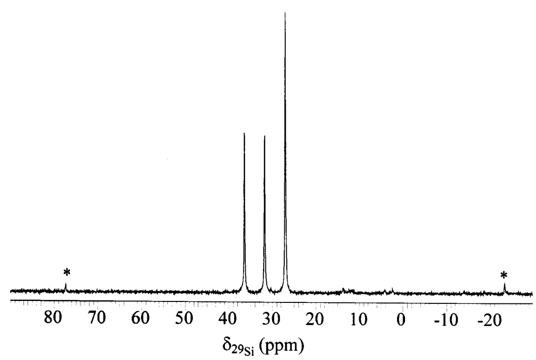

Fig. 6. ^{29}Si-CP-MAS-NMR spectrum of the solid compound **2a** showing two different signals for the two crystallographically different $SiMe_2$ units and one for the central Si_2Me_2 unit.

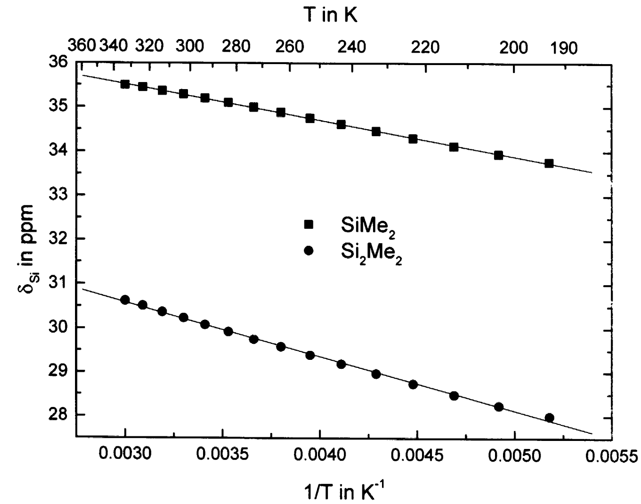

a)

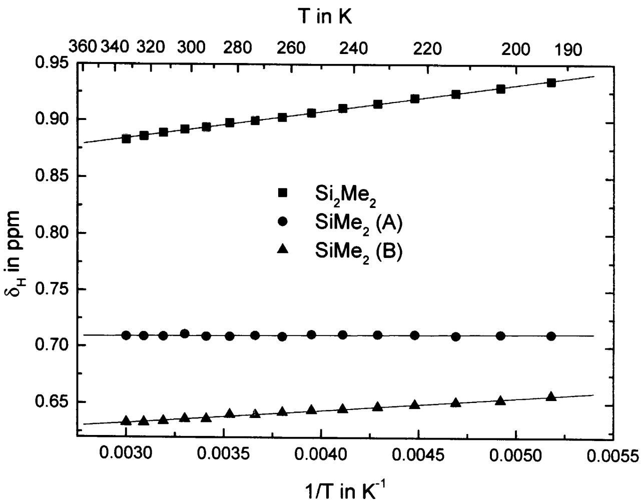

b)

Fig. 7. (a) ^{29}Si-NMR chemical shifts of **2a** as a function of temperature (− 80 to + 60 °C). (b) ^{1}H-NMR chemical shifts of **2a** as a function of temperature (− 80 to + 60 °C).

observed [7]. On the other hand, no intermolecular contacts are formed in the case of the five-membered tin chalcogen heterocycles $^{t}Bu_2Sn(E)_2Sn^{t}_2Bu_4$ (E = S, Se, Te). The bulky ^{t}Bu substituents prevent such contacts, force the five-membered ring into a planar (E = S) or almost planar (E = Se) conformation and increase the Sn–E bond lengths [8].

2.3. *3,7-Dichalcogena-1,2,4,5,6,8-hexasila-bicyclo[3.3.0]octanes* (*5a–c*)

A different class of silchalcogenanes is accessible from the doubly branched hexasilane $(ClMe_2Si)_2$-$SiMeSiMe(SiMe_2Cl)_2$:

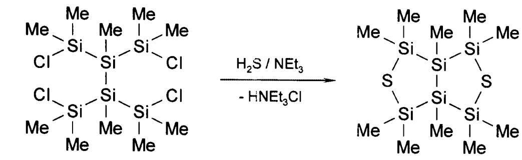

5a

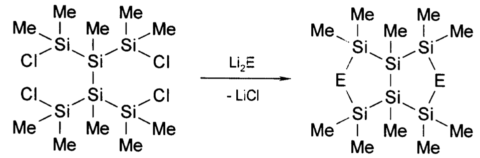

5b : E = Se
5c : E = Te

These reactions are surprisingly clean, no other silicon containing by-products have been observed. These reactions show again the high stability of five-membered rings in these systems even though heterocycles with four silicon and one chalcogen atom are formed.

While we have already published the formation and the molecular structure of the sulfur compound **5a**, see Fig. 9 [4], we now succeeded in the preparation of the selenium (**5b**) and tellurium (**5c**) derivatives. The NMR data of **5a–c** are summarized in Table 7. Remarkable are the relatively drastic changes of the ^{29}Si-NMR chemical shifts of the branching SiMe units from E = S to E = Te even though the first coordination sphere at these silicon atoms remains unchanged. As also observed for other silselenanes and -telluranes [5,9] the ^{125}Te-NMR parameters (δ and $^{1}J_{ESi}$) follow the corresponding ^{77}Se-NMR data of the analogous selenium compounds by a factor of 2.5–2.7.

3. Experimental

3.1. *NMR and GC–MS measurements*

All NMR spectra were recorded on a Bruker DPX 400 in $CDCl_3$ solution and with TMS as internal standard for ^{1}H, ^{13}C and ^{29}Si. External Me_4Sn, Ph_2Se_2 (δ_{Se} 460 ppm) and Ph_2Te_2 (δ_{Te} 422 ppm) in $CDCl_3$ were used as standards for ^{119}Sn, ^{77}Se and ^{125}Te.

In order to obtain a sufficient signal-to-noise ratio of ^{29}Si-NMR spectra for resolving $^{1}J_{SiC}$, $^{1}J_{SiSi}$, $^{1,2}J_{SiSe}$ or $^{1,2}J_{SiTe}$ satellites ^{29}Si INEPT spectra were also recorded. ^{77}Se, ^{125}Te and ^{119}Sn spectra were determined using an IGATED pulse program.

Temperature dependent NMR spectra of **2a** were done in a solution of 60 vol% THF and 40 vol% $CDCl_3$ and TMS as internal standard. ^{1}H- and ^{29}Si-INEPT-NMR spectra were taken over a temperature range from − 80 to + 60 °C in steps of 10 °C.

^{29}Si-CP-MAS-NMR spectra were recorded on a Bruker MSL 300 using the CPCYCL pulse program, spinning frequency 3000 Hz, contact time 5 ms, calibration with external Q_8M_8.

Mass spectra were measured on a Hewlett–Packard 5971 (ionization energy 70 eV, column 30 m × 0.25

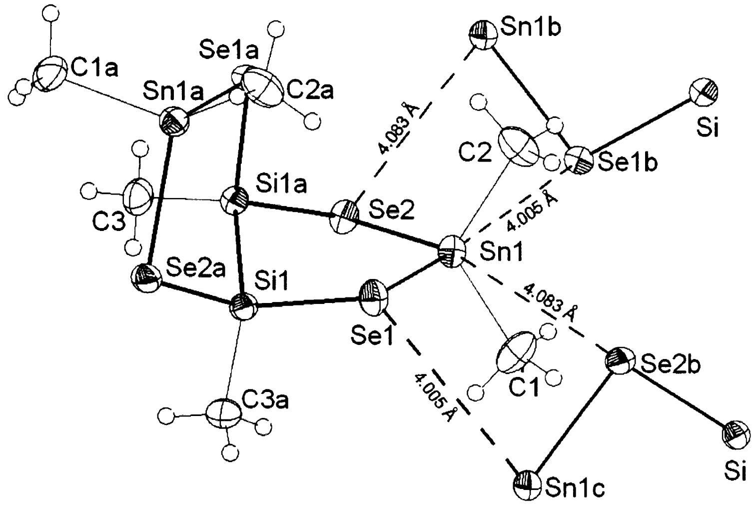

Fig. 8. Intermolecular contacts between tin and selenium in **3c**.

mm × 0.25 μm, phenylmethylpolysiloxane, column temperature 80 °C (3 min)/20 K min^{-1}, He flow of 0.5 ml min^{-1}).

3.2. Crystal structure analyses

X-ray structure analysis measurements were performed on a Bruker SMART CCD. Crystal data of **2b**, **2e** and **3c** as well as data collection and refinement details are given in Table 8.

The unit cell dimensions were determined with the program SMART [10]. For data integration and refinement of the unit cell parameters the program SAINT [10] was used. The space group was determined with the aid of the programs XPREP [10] (**2e** and **3c**) and ABSEN [11] (**2b**). All data were corrected for absorption applying SADABS [12]. The structures were solved using direct methods (SHELX-97 [13] for **2e** and **3c**, SIR97 [14] for **2b**), refined using least-squares methods (SHELX-97) and drawn using ZORTEP [15]. The ellipsoids at the non-hydrogen atoms are at the 50% probability level. The protons of the methyl groups in **2b** could be located but not refined to sufficient quality. They have been generated using the FIX 137 command. Because of the mirror plane in **2b** the hydrogen positions at C2, C4 and C5 are duplicated.

3.3. Theoretical methods

The ab initio molecular orbital calculations were carried out using the GAUSSIAN 98 series of programs [16]. Geometries were fully optimized at the DFT level, using Becke's three-parameter hybrid exchange functional and the correlation functional of Lee et al. (B3LYP) [17,18]. Geometry optimizations, harmonic frequencies, and zero-point vibrational energies were calculated with the polarized 6-31G* basis set for C, H and Si [19,20] and with effective core potentials for Ge, Sn and Se [21]. All structures were identified as true local minima by their Hessian matrices.

3.4. Starting materials

H_2S, Se, Te, triethylamine, 1 M $LiBEt_3H$ in THF (super hydride), Me_2SiCl_2, Me_2GeCl_2, Me_2SnCl_2, Ph_2SnCl_2 were commercially available. Compound **1** [22], $(CH_2)_5C(SH)_2$ [6] and $(ClMe_2Si)_2Si_2Me_2(SiMe_2Cl)_2$ [23] were prepared as described previously. THF was distilled from sodium potassium alloy prior to use. The other solvents were dried over KOH or sodium wire. All reactions were carried out under argon applying standard Schlenk techniques.

3.5. Preparation of $R_2M(S)_2Si_2Me_2(S)_2MR_2$ (2a–d) ($MR_2 = SiMe_2$, $GeMe_2$, $SnMe_2$, $SnPh_2$)

In a typical experiment 2 mmol of the corresponding dichloro compound (Me_2SiCl_2, Me_2GeCl_2, Me_2SnCl_2 or Ph_2SnCl_2) was dissolved in 40 ml of hexane (or toluene in the cases of the organotin chlorides) and 0.456 g (2

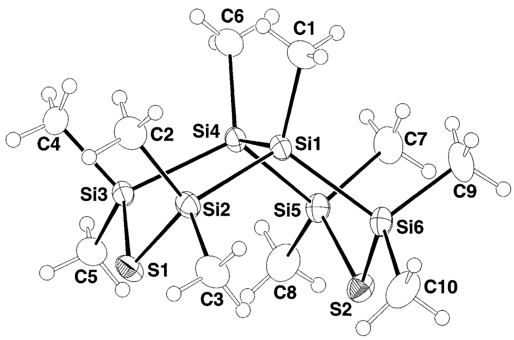

Fig. 9. Molecular structure of **5a** [4].

Table 7
NMR data (ppm, Hz) of the 3,7-dichalcogena-1,2,4,5,6,8-hexasilabicyclo[3.3.0]octanes $E(Me_2Si)_2Si_2Me_2(SiMe_2)_2E$ (E = S, Se, Te (**5a–c**)

compound	δ_E	group	δ_{Si}	$^1J_{SiSi}$	J_{SiE}	δ_C	$^1J_{SiC}$	δ_H
5a 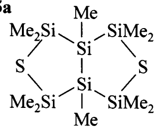	-	SiMe	-71.3	64.1	-	-12.05		0.28
		$SiMe_2$	16.4		-	3.78 / 4.36	45.2	0.49 / 0.54
5b 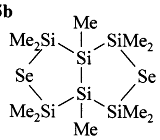	-278	SiMe	-63.7	64.4	^2J: 5.4	-11.3	33.9	0.26
		$SiMe_2$	12.4		^1J 107.9	3.81 / 3.95	43.0	0.59 / 0.65
					^3J 17.1			
5c 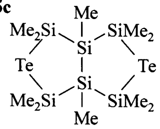	-736	SiMe	-49.8	58.8	^2J 21.4	-10.3		0.87
		$SiMe_2$	-7.6		^1J 270.2	3.42 / 3.91	42.5	1.24

Table 8
Crystal data of **2b**, **2e** and **3c** as well as data collection and refinement details

	2b	**2e**	**3c**
Crystal system	Orthorhombic	Triclinic	Orthorhombic
Space group	*Pnma*	$P\bar{1}$	*Pbcn*
Unit cell dimensions			
a (Å)	12.2673(9)	6.92390(10)	9.81560(10)
b (Å)	9.9225(8)	9.4610(2)	14.2553(2)
c (Å)	13.7735(10)	15.6112(3)	13.1109(2)
α (°)	90	78.0530(10)	90
β (°)	90	85.9290(10)	90
γ (°)	90	71.0050(10)	90
Volume (Å^3); *Z*	1676.5(2); 4	946.01(3); 2	1834.53(4); 4
$D_{calc.}$ (g cm^{-3})	1.663	1.330	2.533
Linear absorption coefficient (mm^{-1})	4.196	0.618	10.762
Radiation used	Mo–K_α	Mo–K_α	Mo–K_α
Temperature (K)	173(2)	173(2)	173(2)
Scan method	ω scans	ω scans	ω scans
Absorption correction	Empirical	Empirical	Empirical
Max/min transmission	0.519/0.487	0.902/0.693	0.119/0.052
Measured reflections	6286	7668	13047
Independent reflections	2517	5143	2715
Observed reflections	2171	3792	2170
R_{int}	0.0206	0.0253	0.0516
θ Range for collection (°)	2.22–30.69	1.33–30.67	2.52–30.84
Completeness to θ_{max} (%)	91.9	88.0	93.9
Refinement method	Full-matrix least-squares on F^2	Full-matrix least-squares on F^2	Full-matrix least-squares on F^2
Final R_1 ($I>2\sigma(I)$)	0.0216	0.0349	0.0278
R_1 (all data)	0.0270	0.0591	0.0405
H-locating and refining	DIFMAP/REFALL	DIFMAP/REFALL	DIFMAP/mixed
Goodness-of-fit on F^2	1.046	1.007	1.081
Max/min e-density (e Å^{-3})	0.436/−0.899	0.381/−0.273	0.961/−1.079

mmol) of compound **1** was added. With stirring, a stream of dried H_2S was passed through the solution while 1.66 ml (12 mmol) of NEt_3 was slowly added by a syringe. A white precipitation of triethylammonium chloride appeared immediately. After stirring for 1 h the mixture was filtered and the solvent removed to yield the bicyclo[3.3.0]octanes as a white crystalline residue. The products were recrystallized from hot saturated solutions in hexanes to give single crystals suitable for X-ray analysis.

2a: m.p. 75–77 °C, **2b**: m.p. 127 °C, **2c**: m.p. 184–187 °C, **2d**: m.p. 130 °C.

2a: GC–MS (*m*/*e*, rel. int.): 330 (M^+, 36), 315 ($Me_5Si_4S_4$, 26), 165 ($Me_3Si_2S_2$, 100), 73 (Me_3Si, 20).

2b: GC–MS: 420 (M^+ ($^{74}Ge^{72}Ge$), 1.5), 405 ($Me_5^{74}Ge^{72}GeSi_2S_4$, 73), 301 ($Me_5^{74}GeSi_2S_3$, 30), 211 ($Me_3^{74}GeSiS_2$, 100), 181 ($Me^{74}GeSiS_2$, 21), 165 ($Me_3Si_2S_2$, 51), 135 ($MeSi_2S_2$, 10), 119 ($Me_3^{74}Ge$, 36), 105 ($Me_3SiS$, 24), 89 ($Me^{74}Ge$, 16), 73 ($Me_3Si$, 74). (The isotopic patterns of all fragments fitted the natural abundance of ^{70}Ge:^{72}Ge:^{73}Ge:^{74}Ge:^{76}Ge = 20.5:27.4:7.8:36.5:7.8 [24].)

2c: Anal. Calc. for $C_6H_{18}S_4Si_2Sn_2$: C, 14.07; H, 3.54; S, 25.05; Found: C, 14.78; H, 3.59; S, 24.89%.

A molar ratio of Me_2MCl_2 to **1** of 1:1 instead of 2:1 was applied in order to prevent the formation of the six-membered heterocycles $(Me_2MS)_3$ as by-products. Under the reaction conditions excess **1** forms the tetracyclic cage compound $Me_6Si_6S_6$ [4], which is insoluble in hexane and can therefore be removed together with the ammonium salt by filtration.

3.6. $(CH_2)_5C(S)_2Si_2Me_2(S)_2C(CH_2)_5$ (2e)

A total of 0.228 g (1 mmol) of compound **1** was dissolved in 40 ml of hexane, 0.296 g (2 mmol) of $(CH_2)_2C(SH)_2$ and 0.55 ml (4 mmol) of NEt_3 were added under stirring. After 1 h the mixture was filtered from the precipitated ammonium salt and the solvent removed to yield **2e** as colorless crystals without any by-products. The product was recrystallized from hot hexane, m.p. 130 °C.

3.7. $Me_2M(E)_2Si_2Me_2(E)_2MMe_2$ (3a–4c) (M = Si, Ge, Sn; E = Se, Te)

3.7.1. Selenium compounds (3a–c)

A total of 0.16 g (2 mmol) of black selenium powder was reacted with a mixture of 4 ml of a 1 M solution of $Li[BEt_3H]$ in THF and an additional 5 ml of THF with stirring. The selenium dissolved within a few seconds with formation of a white suspension of Li_2Se. A mixture of 0.114 g (0.5 mmol) of **1** and 1 mmol of Me_2MCl_2 dissolved in 5 ml of hexane (or toluene in the case of Me_2SnCl_2) was added to the suspension. The precipitation of Li_2Se disappeared almost immediately. After stirring for 30 min at room temperature (r.t.) the solvents were removed in vacuo and replaced by 10 ml of hexane. The solution was separated from precipitated LiCl. Removal of the solvent produced **3a**–**c** as colorless crystalline powders. Crystals of **3c** were grown from toluene solution.

3.7.2. Tellurium compounds (4a–c)

A total of 0.25 g (2 mmol) of tellurium powder (200 mesh) was added to a mixture of 4 ml of a 1 M solution of $Li[BEt_3H]$ in THF and an additional 5 ml of THF under stirring. After 5 min the tellurium started to react with formation of a deep purple solution which became dark red after 1 h at r.t.

As described for the selenium compounds a mixture of 0.114 g (0.5 mmol) of **1** and 1 mmol of Me_2MCl_2 dissolved in 5 ml of hexane (or toluene in the case of Me_2SnCl_2) was added to the Li_2Te suspension. The analogous work-up yielded the tellurium containing bicyclo[3.3.0]octanes **4a**–**c** as light yellow crystalline residues which are extremely air sensitive and turn black within seconds but are stable under argon at r.t. for weeks.

3.8. 3,7-Dichalcogena-1,2,4,5,6,8-hexasilabicyclo[3.3.0]-octanes (5a–c)

The preparation of **5a** starting from the doubly branched hexasilane, H_2S and NEt_3 has already been described in Ref. [4]. The addition of 0.23 g (0.5 mmol) of $(ClMe_2Si)_2Si_2Me_2(SiMe_2Cl)_2$ to a suspension of 1 mmol Li_2Se or Li_2Te (prepared as described above) and work-up as described in Section 3.5 yielded the selenium compound **5b** as relatively low melting point crystalline needles (m.p. 60 °C) and the tellurium derivative **5c** as a light yellow, extremely air sensitive oil.

5a: GC–MS (*m*/*e*, relative intensity): 382 (M^+, 73), 367 ($Me_9Si_6S_2$, 38), 323 ($Me_7Si_5S_2CH_2$, 32), 309 ($Me_7Si_5S_2$, 61), 277 (Me_7Si_5S, 13), 249 (Me_7Si_4S, 19), 131 (Me_5Si_2, 16), 73 (Me_3Si, 100), 59 (Me_2SiH, 15).

5b: GC–MS: 478 (M^+, 19), 463 ($Me_9Si_6{}^{80}Se_2$, 15), 419 ($Me_7Si_5{}^{80}Se_2CH_2$, 9), 405 ($Me_7Si_5{}^{80}Se_2CH_2$, 13), 325 ($Me_7Si_5{}^{80}Se$, 14), 297 ($Me_7Si_4{}^{80}Se$,11), 267 ($Me_5Si_4{}^{80}Se$, 6), 239 ($Me_5Si_3{}^{80}Se$, 7), 159 (Me_5Si_3, 11), 131 (Me_5Si_2, 23), 73 (Me_3Si, 100), 59 (Me_2SiH, 12). (The isotopic patterns of all fragments fitted the natural abundance of ^{76}Se:^{77}Se:^{78}Se:^{80}Se:^{82}Se = 9.2:7.6:23.7:49.8:8.8 [24].)

4. Supplementary material

Crystallographic data for the structural analysis have been deposited with the Cambridge Crystallographic Data Centre, CCDC no. 163663 for compound **2b**, CCDC no. 163664 for compound **2e** and CCDC no. 163665 for compound **3c**. Copies of this information may be obtained free of charge from The Director, CCDC, 12 Union Road, Cambridge CB2 1EZ, UK (Fax: +44-1223-336033; e-mail: deposit@ccdc.cam.ac.uk or www: http://www.ccdc.cam.ac.uk).

Acknowledgements

The authors thank the Deutsche Forschungsgemeinschaft for financial support. Special thanks are given to the Computing Centre of the TU Bergakademie Freiberg for supplying disk space and computing time. Furthermore, the authors thank Prof. H. Lang, Chair of Inorganic Chemistry, TU Chemnitz for the access to the X-ray facility used to determine the single-crystal structures.

References

[1] J.C.J. Bart, J.J. Daly, J. Chem. Soc. Dalton Trans. (1975) 2063.
[2] W. Ando, T. Kadowaki, Y. Kabe, M. Ishii, Angew. Chem. Int. Ed. Engl. 31 (1992) 59.
[3] M. Unno, Y. Kawai, H. Shioyama, H. Matsumoto, Organometallics 16 (1997) 4428.
[4] U. Herzog, U. Böhme, G. Roewer, G. Rheinwald, H. Lang, J. Organomet. Chem. 602 (2000) 193.
[5] U. Herzog, G. Rheinwald, J. Organomet. Chem. 627 (2001) 23.
[6] J. Jentzsch, J. Fabian, R. Mayer, Chem. Ber. 95 (1962) 1764.
[7] M. Dräger, B. Mathiasch, Z. Anorg. Allg. Chem. 470 (1980) 45.
[8] H. Puff, B. Breuer, W. Schuh, R. Sievers, R. Zimmer, J. Organomet. Chem. 332 (1987) 279.
[9] U. Herzog, G. Rheinwald, J. Organomet. Chem. 628 (2001) 133.
[10] Bruker AXS Inc., Madison, WI, USA, 1998.
[11] P. McArdle, J. Appl. Crystallogr. 29 (1996) 306.
[12] SADABS: Area-Detector Absorption Correction, Siemens Industrial Automation, Inc., Madison, WI, USA, 1996.
[13] G.M. Sheldrick, SHELX-97 [Includes SHELXS-97, SHELXL-97, CIFTAB]. Programs for Crystal Structure Analysis (Release 97-2), University of Göttingen, Germany, 1997.
[14] A. Altomare, M.C. Burla, M. Camalli, G.L. Cascarano, C. Giacovazzo, A. Guagliardi, A.G.G. Moliterni, G. Polidori, R. Spagna, J. Appl. Crystallogr. 32 (1999) 115.
[15] L. Zsolnai, G. Huttner, ZORTEP, University of Heidelberg, Germany, 1994.
[16] M.J. Frisch, G.W. Trucks, H.B. Schlegel, G.E. Scuseria, M.A. Robb, J.R. Cheeseman, V.G. Zakrzewski, J.A. Montgomery Jr., R.E. Stratmann, J.C. Burant, S. Dapprich, J.M. Millam, A.D. Daniels, K.N. Kudin, M.C. Strain, O. Farkas, J. Tomasi, V. Barone, M. Cossi, R. Cammi, B. Mennucci, C. Pomelli, C. Adamo, S. Clifford, J. Ochterski, G.A. Petersson, P.Y. Ayala, Q. Cui, K. Morokuma, D.K. Malick, A.D. Rabuck, K. Raghavachari, J.B. Foresman, J. Cioslowski, J.V. Ortiz, B.B. Stefanov, G. Liu, A. Liashenko, P. Piskorz, I. Komaromi, R. Gomperts, R.L. Martin, D.J. Fox, T. Keith, M.A. Al-Laham, C.Y. Peng, A. Nanayakkara, C. Gonzalez, M. Challacombe, P.M.W. Gill, B. Johnson, W. Chen, M.W. Wong, J.L. Andres, C. Gonzalez, M. Head-Gordon, E.S. Replogle, J.A. Pople, GAUSSIAN 98, Revision A.6, Gaussian Inc, Pittsburgh, PA, USA, 1998.
[17] A.D. Becke, J. Chem. Phys. 98 (1993) 5648.
[18] P.J. Stephens, F.J. Devlin, C.F. Chabalowski, M.J. Frisch, J. Phys. Chem. 98 (1994) 11623.
[19] P.C. Hariharan, J.A. Pople, Theor. Chim. Acta 28 (1973) 213.
[20] M.M. Francl, W.J. Pietro, W.J. Hehre, J.S. Binkley, M.S. Gordon, D.J. DeFrees, J.A. Pople, J. Chem. Phys. 77 (1982) 3654.
[21] W.R. Wadt, P.J. Hay, J. Chem. Phys. 82 (1985) 284.
[22] R. Lehnert, M. Höppner, H. Kelling, Z. Anorg. Allg. Chem. 591 (1990) 209.
[23] G. Kollegger, K. Hassler, J. Organomet. Chem. 485 (1995) 233.
[24] J. Emsley, Die Elemente, Walter de Gruyter, Berlin, New York, 1994.